

See discussions, stats, and author profiles for this publication at: <https://www.researchgate.net/publication/231403118>

# Hydrocarbon trapping and condensation on platinum (111)

ARTICLE *in* THE JOURNAL OF PHYSICAL CHEMISTRY · OCTOBER 1992

Impact Factor: 2.78 · DOI: 10.1021/j100201a008

---

CITATIONS

13

---

READS

7

2 AUTHORS, INCLUDING:



Bruce Koel

Princeton University

296 PUBLICATIONS 9,043 CITATIONS

SEE PROFILE

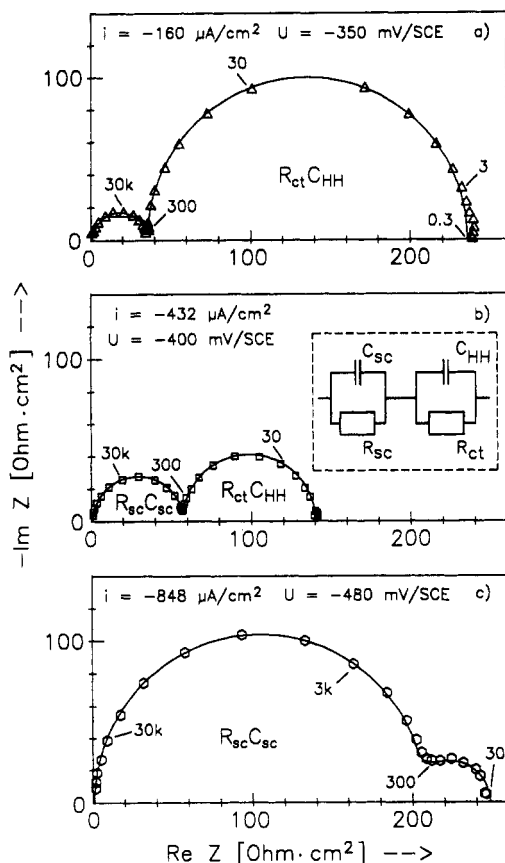


**Figure 4.** Impedance data for p-InP in 1 M H<sub>2</sub>SO<sub>4</sub> (N<sub>2</sub>) at a constant illumination intensity ( $i_{ph} \approx -1.0$  mA/cm<sup>2</sup>) and varying current densities  $i$ . Measurement points and fitted curves; the fitting parameters to the circuit in the insert are listed in Table I.

thought to be achieved by a self-stabilization process due to a current-dependent growth of (and light absorption in) the In layer. Mott-Schottky data precision is mainly based on a low concentration of bulk trap states.<sup>12</sup>

Attempts to verify Mott-Schottky and impedance data of the p-InP-In Schottky contact after removing the electrode from the electrolyte were not successful, probably due to an insufficient contact of the In layer to the used metal contact grid (In layer

thickness  $\approx 10$ –30 monolayers as derived from the oxidation transients). The photovoltage  $U_{ph}$  could be reproduced ( $U_{ph} \approx 450$  mV at  $\approx 200$  mW/cm<sup>2</sup> illumination intensity).

In conclusion, the corrosion of bare p-InP under H<sub>2</sub> evolution conditions leads to the formation of an almost ideal p-InP-In Schottky contact with a large barrier height at the semiconductor surface. Under illumination, the resulting p-InP-In/electrolyte contact shows typical features known also from other semiconductor electrodes such as an S-shaped  $i/U$  curve, shifts of Mott-Schottky curves, and a two-time constant impedance response. One might therefore ask whether the above-discussed model is valid in a more general sense (cf. ref 16) although frequency dispersion phenomena and small differential  $C_{HH}$  values<sup>8,9,17</sup> may complicate the evaluation of experimental data.

Achieved data precision emphasizes the suitability of (photo)electrochemical characterization methods as an alternative to conventional solid-state characterization of semiconductor materials.

**Acknowledgment.** This work was part of the Fundamental Research Program in the German/Saudi-Arabian project HY-SOLAR.

## References and Notes

- (1) Aharon-Shalom, E.; Heller, A. *J. Electrochem. Soc.* **1982**, *129*, 2865.
- (2) Szklarczyk, M.; Bockris, J. O'M. *J. Phys. Chem.* **1984**, *88*, 5241.
- (3) Schneemeyer, L. F.; Heller, A.; Miller, B. In *Semiconductor Electrodes*; Finklea, H. O., Ed.; Elsevier: Amsterdam, 1988; pp 411–456.
- (4) Menezes, S.; Miller, B.; Bachmann, K. *J. Vac. Sci. Technol. B* **1983**, *1*, 48.
- (5) Gorochov, O.; Stoicoviciu, L. *J. Electrochem. Soc.* **1988**, *135*, 1159.
- (6) Gagnaire, A.; Joseph, J.; Etcheberry, A.; Gautron, J. *J. Electrochem. Soc.* **1985**, *132*, 1655.
- (7) Kühne, H.-M.; Schefold, J. *J. Electrochem. Soc.* **1990**, *137*, 568.
- (8) Schefold, J.; Kühne, H.-M. *J. Electroanal. Chem.* **1991**, *300*, 211.
- (9) Schefold, J. *J. Electroanal. Chem.*, in press.
- (10) Erdey-Grúz, T. *Kinetik der Elektrodenprozesse*; Akadémiai Kiadó: Budapest, 1975; pp 173, 204.
- (11) Pourbaix, M. *Atlas d'Equilibres Electrochimiques*; Gauthiers-Villars: 1963; p 438.
- (12) Rhoderick, E. H.; Williams, R. H. *Metal-Semiconductor Contacts*; Monographs in Electrical and Electronic Engineering; Clarendon Press: Oxford, 1988.
- (13) Ismail, A.; Ben Brahim, A.; Palau, J. M.; Lassabatière, L.; Lindau, I. *Vacuum* **1986**, *36*, 217.
- (14) Gärtner, W. W. *Phys. Rev.* **1959**, *116*, 84.
- (15) Werner, J. H. In *Metallization & Metal-Semiconductor Interfaces*; Batra, I. P., Ed.; Plenum Press: New York, 1989; pp 235–255.
- (16) Kumar, A.; Santangelo, P. G.; Lewis, N. S. *J. Phys. Chem.* **1992**, *96*, 834.
- (17) Chazalviel, J.-N. *J. Electrochem. Soc.* **1982**, *129*, 963.

## Hydrocarbon Trapping and Condensation on Pt(111)

L. Q. Jiang and Bruce E. Koel\*

Department of Chemistry, University of Southern California, Los Angeles, California 90089  
(Received: July 20, 1992; In Final Form: September 9, 1992)

A direct, reflected beam method under ultrahigh-vacuum conditions was used to measure the sticking coefficient of several small hydrocarbon molecules (methylcyclohexane, cyclohexane, toluene, benzene, and methanol) on clean and adsorbate-covered Pt(111) surfaces and on the molecular solid phases that can be formed at temperatures below that required for multilayer sublimation. We find that the sticking coefficient for all of these molecules on the clean Pt(111) surface and the molecular solid phase at 100 K is unity. The simple, classical hard-cube model provides a useful way to understand this behavior.

One of the most fundamental pieces of information in understanding reaction mechanisms in heterogeneous catalysis is knowledge of the trapping probability on clean and adsorbate-covered metal surfaces. In particular, hydrocarbon conversion reactions on Pt catalysts often involve elementary reaction steps

for adsorption of alkanes and alkenes. It is surprising therefore that few direct measurements of sticking coefficients of hydrocarbons on Pt surfaces are available. Molecular beam studies by Madix and co-workers<sup>1,2</sup> for CH<sub>4</sub> and C<sub>2</sub>H<sub>6</sub> adsorption and dissociation dynamics on Pt(111) at 95 K indicate (by extrapolation

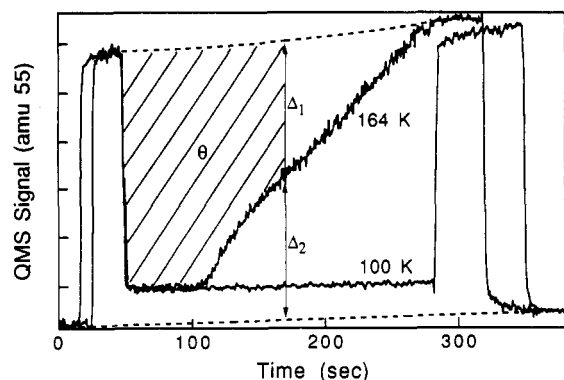


Figure 1. Direct sticking coefficient measurement for MCH adsorption on clean Pt(111) at 100 and 164 K.

of their results) that the sticking probability at the low kinetic energies ( $\approx 1.2$  kJ/mol) characteristic of 300 K gas would be unity or near unity. However, recent papers by Rodriguez and Campbell<sup>3</sup> reported that the sticking coefficient and condensation probability (to form the solid phase) of several small hydrocarbons (benzene, cyclohexane, cyclopentene) on Pt(111) at 100 K was about 0.25. While this value seems too small according to conventional wisdom, the authors point out correctly that no data existed to discount their result. Here we present a study of the sticking coefficient of methylcyclohexane (MCH), cyclohexane, toluene, benzene, and methanol on the clean and adsorbate-covered Pt(111) surfaces at 100 K. We used a direct method for making these measurements that is due to King and Wells<sup>4</sup> and used in the more recent molecular beam studies of Madix and co-workers.<sup>1</sup>

The experiments are performed in an ultrahigh-vacuum (UHV) chamber with a base pressure of  $4 \times 10^{-11}$  Torr. The apparatus has been described before.<sup>5</sup> The Pt(111) crystal can be cooled to 95 K using liquid nitrogen or resistively heated to 1200 K. The temperature is monitored with a chromel–alumel thermocouple spot-welded to the side of the crystal. The Pt(111) surface is cleaned by argon ion sputtering and annealing, followed by heating to 1000 K in  $2 \times 10^{-8}$  Torr of  $O_2$  until no impurities can be detected by Auger electron spectroscopy (AES). All of the reagents, i.e., MCH, cyclohexane, toluene, benzene, and methanol, are of research purity and are placed separately in Pyrex containers along with dried molecular sieve granules to adsorb  $H_2O$ . The vapor of the room temperature liquids is used for adsorption and is purified by freeze, pump, and thaw cycles. The purity of all of the gases is proven by gas chromatography and by in-situ mass spectrometry.

The chamber is equipped with a collimated multicapillary array beam doser and a UTI-100C quadrupole mass spectrometer (QMS) with its ionizer capped with an aperture for line-of-sight temperature-programmed desorption (TPD). The QMS is shielded and far away from the doser so that it detects only the random flux of molecules effusing into the chamber from the doser. A 2- $\mu$ m-diameter, conductance-limiting orifice mounted in the doser assembly separates the UHV system from the doser backing pressure of  $\approx 1$  Torr, which is measured by a 0–10-Torr Baratron pressure gauge. A 280-cm<sup>3</sup> ballast in the backing line stabilizes the pressure while dosing and thereby ensures a constant beam flux. The 1.04-cm-diameter glass microcapillary array, composed of closely spaced 25- $\mu$ m-i.d. cylinders of 1-mm length, is mounted in a stainless steel cap with a 0.5-cm-diameter aperture. This smaller source diameter, compared to the Pt(111) crystal diameter of 1 cm, and the short distance of approximately 0.3 cm between the doser and the crystal ensure a large fraction of the beam ( $\approx 87\%$ ) impinging on the crystal and thus a large dynamic range and high precision for the measurements of  $S$ .

The absolute sticking coefficient,  $S$ , is measured directly using a method based on beam reflection where the sample acts as a getter for the incident effusive beam from the collimated microcapillary array beam doser. Figure 1 illustrates this method for MCH adsorption on Pt(111) at 100 and 164 K, respectively. The mass 55 cracking fragment of MCH is used to monitor the

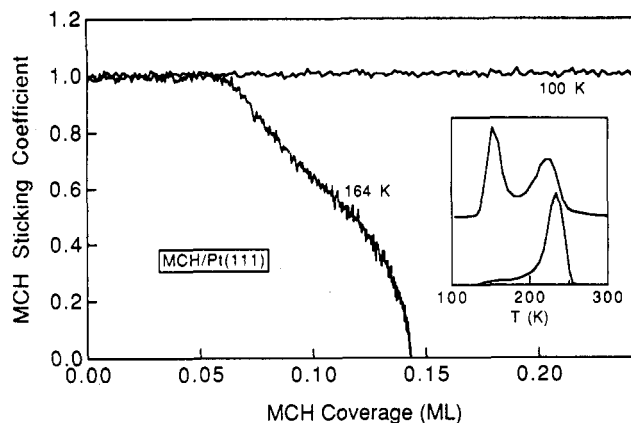


Figure 2. MCH sticking coefficient versus coverage for MCH adsorption on clean Pt(111) at 100 and 164 K. The inset shows the TPD spectra for MCH desorbing from Pt(111) after 65- and 230-s exposure to MCH on the surface at 100 K.

partial pressure of MCH. After the MCH beam is turned on (indicated by the initial rise of both curves) and stabilized, the Pt(111) sample is quickly rotated into the beam, causing a sharp drop in  $P$  at  $t \approx 50$  s at both 100 and 164 K due to the uptake of MCH by Pt(111). The dashed line above the pressure–time curve at 164 K is constructed to approximate the behavior expected if  $S = 0$  or the sample is out of the beam. Justification of our construction of the smooth dashed line has been discussed.<sup>5</sup> Since the sample holder is at 100 K in both experiments and only the Pt is heated for the 164 K experiment, the possibility of partly measuring the condensation on the sample holder is ruled out. This is further supported by the fact that the dashed line is followed when Pt is heated to above 300 K. The sticking coefficient at a coverage of  $\theta$  (indicated by the area in Figure 1 for  $T = 164$  K) is obtained by  $S = \Delta_1 / F(\Delta_1 + \Delta_2)$  from this experiment. Here  $F$  is the fraction of the beam that impinges onto the sample, and it can be either calculated or determined experimentally.<sup>6</sup> The calculated value of  $F$  for our sample-doser geometry agrees well with the experimental value of 0.87 determined by comparing our data for CO adsorption on clean Pt(111) at room temperature to the known sticking coefficient of this system.<sup>7</sup> Using this value of  $F$ , we can directly evaluate the sticking coefficients for the adsorption of MCH and other hydrocarbon molecules. Figure 1 clearly shows that  $S$  is unity and independent of coverage for MCH adsorption on Pt(111) at 100 K, at least for an exposure time of 230 s at which point the sample is rotated out of the beam. Multilayer desorption is seen in the MCH TPD described below after this exposure. We have done adsorption experiments at 100 K for exposure times exceeding 520 s, and again  $S$  is unity and independent of coverage. The hydrocarbon coverage  $\theta_{HC}$  was calibrated using the known saturation coverage of 0.5 monolayer (ML) for CO on clean Pt(111) at 300 K.<sup>7</sup> Since  $\theta_{HC} = I_{HC} \int S_{HC} dt$  and  $\theta_{CO} = I_{CO} \int S_{CO} dt$ , and the beam flux  $I \propto P/\sqrt{m}$  where  $m$  is the molecular weight, then

$$\theta_{HC} = \frac{P_{HC}}{P_{CO}} \left( \frac{m_{CO}}{m_{HC}} \right)^{1/2} \frac{\int S_{HC} dt}{\int S_{CO} dt} \theta_{CO} \quad (1)$$

Using eq 1, the room temperature saturation coverage of toluene on Pt(111) is determined to be 0.114 ML (defined relative to Pt(111) surface density of 1 ML =  $1.505 \times 10^{15}$  species/cm<sup>2</sup>), which agrees well with that obtained by Tsai and Muettetieries<sup>8</sup> and Abon et al.<sup>9</sup> using other independent methods.

As shown in Figure 2, when MCH is adsorbed at 164 K on clean Pt(111), the sticking coefficient is unity almost to half coverage, suggesting a strong effect of a precursor state in the adsorption mechanism. At higher coverage  $S$  slowly drops to zero as a monolayer is formed. Considering the limited beam uniformity across the sample and the adsorption/desorption equilibrium that may be set up under the flux of the doses at high coverages,  $S$  might actually be unity to an even larger coverage,

and therefore a stronger precursor effect could be deduced. The low saturation coverage of 0.14 ML at 164 K is a result of the large size of MCH relative to Pt. Multilayers of MCH do not form at 164 K, but the condensation of MCH to form a solid phase does occur at 100 K. This is clear from the inset to Figure 2 which shows the TPD spectra for MCH desorbing from Pt(111) after 65- and 230-s exposure to MCH on the surface at 100 K. MCH coverages of 0.13 and above result in the formation of a MCH desorption peak near 155 K. This peak continues to grow with MCH coverage without saturating, and it is attributed to condensed multilayer MCH. Using the desorption temperature of 155 K appropriate for a coverage in this state of about 1 ML and the heating rate of 10 K/s used in TPD, first-order Redhead analysis yields an activation energy for desorption of 38 kJ/mol, which can be taken as a good estimate of the sublimation energy of pure MCH. The MCH desorption peak near 230 K is due to the reversibly adsorbed MCH monolayer, and the desorption activation energy for this process is about 56 kJ/mol. These values should also be the heats of adsorption into the two states since adsorption occurs readily at 100 K and little or no activation energy is required for adsorption.

Figure 2 also shows that the initial sticking coefficient on the clean Pt(111) surface is independent of temperature between 100 and 164 K.  $S$  is unity for the condensation of at least several monolayers equivalent coverage in the multilayer solid phase of MCH. We found the same behavior for MCH on K- or C-covered Pt(111) surfaces. The unity sticking coefficient for chemisorption onto clean and adsorbate-covered Pt(111) and subsequent condensation into the second and multilayer solid phase at 100 K is also seen for cyclohexane, toluene, benzene, and methanol. The same results have also been obtained recently for butane, isobutane, and isobutylene in our laboratories.

A comparison of our results to those of Rodriguez and Campbell<sup>3</sup> is required. They measured a constant sticking and condensation coefficient of 0.25 independent of coverage for the adsorption of benzene, cyclohexane, and cyclopentene on Pt(111) at 100 K using an indirect method for determining  $S$ . They measured the coverage as a function of exposure and obtained  $S$  by differentiation of the resulting curve. The coverage was determined by XPS and TPD measurements, and the exposure was measured by the ion gauge and elapsed time. While many investigators have used this method, it is well-known that the systematic errors in both the coverage and exposure measurements can be large (although good precision can be obtained). On the basis of our results, we presume that the sticking and condensation coefficients of cyclopentene on Pt(111) at 100 K are also unity.

Condensation of molecules to form a bulk solid phase is often assumed to occur with unit probability, but it is less obvious to assume such high values for adsorption into the first monolayer on a metal surface. The hard-cube model<sup>1,10</sup> is frequently used to analyze the incident beam energy ( $E$ ) and surface temperature ( $T$ ) dependence of the trapping probability of gases on surfaces. In this model, the incident molecule of energy  $E$  and mass  $M$  is accelerated by an attractive, one-dimensional square well potential of depth  $D$  in front of the surface to a velocity of  $u$ :

$$u = -[2(E + D)/M]^{1/2} \quad (2)$$

After collision with the surface cube moving with a velocity  $v$  and mass  $m = M/\mu$ , the gas molecule will be reflected with a velocity of  $u'$ :

$$u' = \frac{u(\mu - 1) + 2v}{\mu + 1} \quad (3)$$

Trapping occurs when  $u' < (2D/M)^{1/2}$ . Thus, the gas molecule will get trapped after it collides with a surface cube that has a velocity smaller than  $v_c$  which is given by

$$v_c = \frac{\mu + 1}{2} \left( \frac{2D}{M} \right)^{1/2} + \frac{\mu - 1}{2} \left[ \frac{2(E + D)}{M} \right]^{1/2} \quad (4)$$

Using  $P(v) = (v - u) \exp(-a^2 v^2)$ , where  $a^2 = m/2kT$ , as the

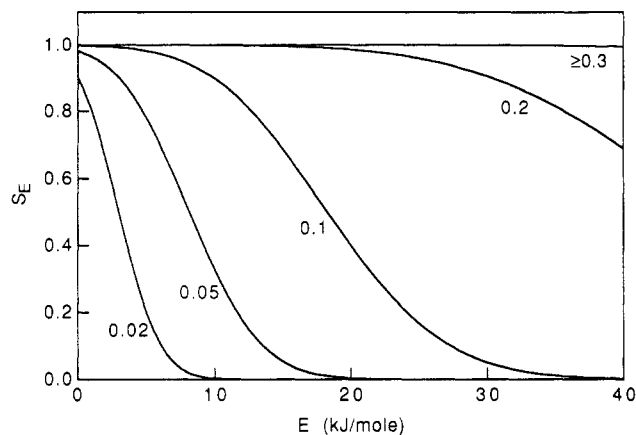


Figure 3. Plot of  $S_E$  as a function of  $E$  for indicated  $\mu$  with  $D = 37.6$  kJ/mol.

probability function of surface velocity at which collision occurs,<sup>11</sup> the trapping probability can be written as

$$S_E = \frac{\int_u^{v_c} (v - u) \exp(-a^2 v^2) dv}{\int_u^{\infty} (v - u) \exp(-a^2 v^2) dv} \quad (5)$$

which results in the following simple expression

$$S_E = \frac{\text{erf}(av_c) + \text{erf}(-au) + (au\sqrt{\pi})^{-1} [\exp(-a^2 v_c^2) - \exp(-a^2 u^2)]}{1 + \text{erf}(-au) - (au\sqrt{\pi})^{-1} \exp(-a^2 u^2)} \quad (6)$$

where erf is the error function. We used  $u$  as the lower limit of the integrations in eq 5 because the gas molecule cannot collide with a surface cube moving with a velocity less than  $u$ . Previous authors<sup>1,10</sup> have carried out the integration from  $-\infty$  instead of  $u$ , probably because it often does not introduce a significant error. Actually, in most cases  $-au \geq 1$  so that eq 6 becomes equivalent to the expression derived in refs 1 and 10. Significant difference can be found, however, in cases of small values of  $-au$  such as occur for large  $\mu$ , high surface temperature, low incident beam energy, and weak adsorption.

Figure 3 shows the plot of  $S_E$  as a function of  $E$  for various  $\mu$  with  $T = 100$  K and  $D = 38$  kJ/mol corresponding to the condensation energy of MCH and the lower limit of MCH adsorption energy on any surfaces as determined from TPD experiments. The thermally averaged sticking coefficient can be obtained by a convolution of  $S_E$  with the flux distribution of energies in the thermal source. For the room temperature ( $T_g = 300$  K) effusive beam used in our experiment, more than 95% of the gas molecules have energies less than 5 kJ/mol. For  $\mu > 0.1$ , which is valid (up to an effective mass of five surface atoms) for MCH adsorption on clean, C- or K-covered Pt(111) surfaces and subsequent condensation, Figure 3 clearly shows that  $S_E$  is unity within a few percent for  $E < 5$  kJ/mol so that the thermal, room temperature gas sticking coefficient will also be near unity. The unity sticking and condensation coefficient of other room temperature or low-energy hydrocarbon molecules on Pt(111) at 100 K can be explained similarly. This primitive explanation does not even require any internal energy considerations, e.g., translational to vibrational and rotational energy transfer that would be appropriate for molecules, certainly these hydrocarbons, that would serve to increase the sticking coefficient.

We would like to make one additional comment. The effective surface mass may be significantly larger than that of the surface atom at low incident translational energy of the gas molecule, in which case the interaction time is long enough to allow cooperative motion among the neighboring atoms. This energy dependence of the surface mass is clearly seen in the study of ethane adsorption on Pt(111)<sup>2</sup> where a constant  $\mu$  will not fit the experimental data over the energy range 0–50 kJ/mol. Better agreement was found

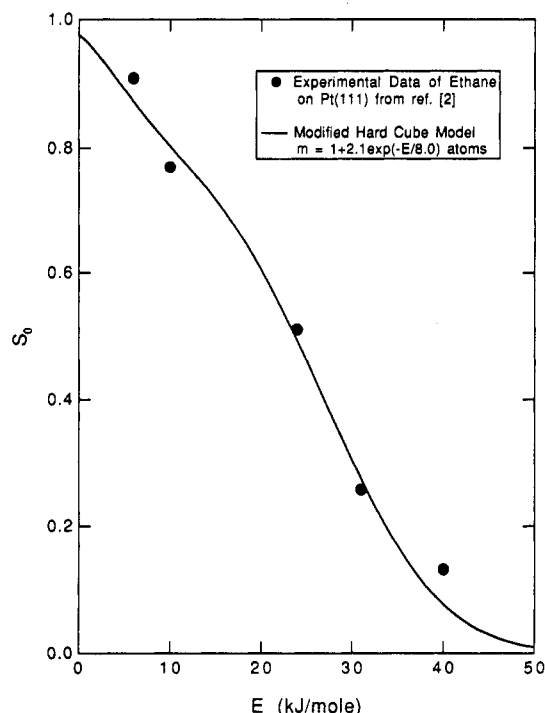


**Figure 4.** Fit of eq 6 to the experimental data of ethane on Pt(111) (taken from Figure 5 in ref 2) with an exponentially decreasing effective surface mass.

for a linearly decreasing effective mass as a function of energy, but this is still not quite satisfactory. The effective surface mass is known to be the same as that of the surface atom at high incident energies as clearly seen in ion scattering experiments. Thus,  $m = 1 + \alpha e^{-E/\beta}$  surface atoms will give the correct effective mass at high energies and therefore is preferred rather than a linearly decreasing effective mass. Using  $\alpha$  and  $\beta$  as fitting parameters and the well depth of 32 kJ/mol for ethane on Pt(111) as experimentally determined by TPD, eq 6 with  $\alpha = 2.1$  and  $\beta = 8$  gives an improved fit to data of Madix et al.,<sup>2</sup> as shown in Figure 4.

The detailed dynamics of sticking could be far more complicated than that implied in the simple hard-cube model, and eq 6 is by

no means a universal expression. For example, the initial sticking coefficient of thermal ( $T_g$  from 30 to 600 K) Ne on Ru(001)<sup>12</sup> is measured to be less than 0.1 and can only be explained by a quantum effect (zero phonon scattering). Nevertheless, the simple, classical hard-cube model seems to be all that is required for our data and provides a useful way to understand hydrocarbon trapping and condensation on metals.

These results provide an important benchmark for improving our understanding of adsorption kinetics and dynamics at solid surfaces. We show that under conditions that the solid phase is thermodynamically stable, i.e., in UHV at 100 K, the condensation coefficient of several small hydrocarbon molecules onto the solid molecular phase is unity. The sticking coefficient of these small hydrocarbons on clean Pt(111) at 100 K is also unity, indicating that mass matching effects are not important at the low translational and internal energies characteristic of room temperature gases.

**Acknowledgment.** This work was partially supported by the U.S. Department of Energy, Office of Basic Energy Sciences, Chemical Sciences Division. B.E.K. gratefully acknowledges the support of a Research Fellowship from the Alfred P. Sloan Foundation.

**Registry No.** Pt, 7440-06-4; PhMe, 108-88-3; C<sub>6</sub>H<sub>6</sub>, 71-43-2; MeOH, 67-56-1; methylcyclohexane, 108-87-2; cyclohexane, 110-82-7.

## References and Notes

- (1) Arumainayagam, C. R.; McMaster, M. C.; Schoofs, G. R.; Madix, R. *J. Surf. Sci.* **1989**, *222*, 213.
- (2) Arumainayagam, C. R.; Schoofs, G. R.; McMaster, M. C.; Madix, R. *J. Phys. Chem.* **1991**, *95*, 1041.
- (3) Rodriguez, J. A.; Campbell, C. T. *J. Phys. Chem.* **1989**, *93*, 826 and references therein.
- (4) King, D. A.; Wells, M. G. *Surf. Sci.* **1972**, *29*, 454.
- (5) Jiang, L. Q.; Koel, B. E.; Falconer, J. L. *Surf. Sci.* **1992**, *273*, 273.
- (6) Winkler, A.; Yates, J. T., Jr. *J. Vac. Sci. Technol.* **1988**, *A6*, 2929.
- (7) Campbell, C. T.; Ertl, G.; Kuipers, H.; Segner, J. *Surf. Sci.* **1981**, *107*, 207.
- (8) Tsai, M. C.; Muetterties, E. L. *J. Am. Chem. Soc.* **1982**, *104*, 2534.
- (9) Abon, M.; Bertolini, J. C.; Billy, J.; Massardier, J.; Tardy, B. *Surf. Sci.* **1985**, *162*, 395.
- (10) Kuipers, E. W.; Tenner, M. G.; Spruit, M. E. M.; Kleyn, A. W. *Surf. Sci.* **1988**, *205*, 241.
- (11) Grimmelmann, E. K.; Tully, J. C.; Cardillo, M. J. *J. Chem. Phys.* **1980**, *72*, 1039.
- (12) Schlichting, H.; Menzel, D.; Brunner, T.; Brenig, W.; Tully, J. C. *Phys. Rev. Lett.* **1988**, *60*, 2515.

## Self-Assembled Ion-Pair Complexes between Porphyrins and Bipyridinium Species: Picosecond Dynamics of Charge Recombination

Stephan L. Logunov<sup>†</sup> and Michael A. J. Rodgers\*

Center for Photochemical Sciences, Department of Chemistry, Bowling Green State University, Bowling Green, Ohio 43403 (Received: July 28, 1992; In Final Form: September 11, 1992)

Spontaneous ion pairing occurs between soluble anionic porphyrins (TPPS and Up) and cationic bipyridinium salts in water. After photoexcitation (532 nm) of the porphyrin component, nonfluorescent ion pairs are formed by fast electron transfer (<100 fs) from the porphyrin donor to the bipyridinium acceptor. The system returns to the ground state by reverse electron transfer without dissociation into separated radical ions. The reverse electron transfer reactions occur over hundreds of picoseconds, and the rate constants are shown to form a homogeneous set of data which demonstrate an inverted region in the driving force range 0.8–1.7 eV. These results are discussed in terms of adiabatic and nonadiabatic electron-transfer theory.

## Introduction

The study of reactions involving the transfer of an electron between molecular entities has occupied the attention of re-

searchers for decades at both theoretical and experimental levels.<sup>1</sup> In this area, important advances began to be made when molecular systems were constructed that contained both donor (D) and acceptor (A) moieties, which constrained them at fixed distance and orientation to each other. Thus, the reaction became intramolecular, and the potentially confusing effects of molecular diffusion were eliminated. Furthermore, the employment of

<sup>†</sup> Permanent address: Biophysics Department, Faculty of Biology, M. V. Lomonosov State University, 119899 Moscow, Russia.

\* To whom correspondence should be addressed.